

# LncRNA SNHG20 enhances the progression of oral squamous cell carcinoma by regulating the miR-29a/DIXDC1/Wnt regulatory axis

Z.-F. CHEN, Y. WANG, L.-L. SUN, S.-Y. DING, H. JINAG

Department of Anesthesiology, Shanghai Ninth People's Hospital, Shanghai JiaoTong University School of Medicine, Shanghai, P.R. China

**Abstract. – OBJECTIVE:** Oral squamous cell carcinoma (OSCC) comprises approximately ~90% of all oral malignancies and exhibits a significant mortality rate worldwide. Although the dysregulation of small nucleolar RNA host gene 20 (SNHG20) participates in the development of multiple malignancies, the molecular mechanisms underlying its regulation of OSCC progression remain to be fully elucidated.

**PATIENTS AND METHODS:** The expression levels of SNHG20, microRNA-29a (miR-29a), and Disheveled-Axin Domain Containing 1 (DIXDC1) were detected by Real Time-quantitative Polymerase Chain Reaction (RT-qPCR). The protein expression levels of DIXDC1 and  $\beta$ -catenin were measured by Western blotting. In addition, MTT assay was performed to measure the cell proliferation ability in SCC9 and SCC15 cells. Cell migration and invasion abilities were measured by wound healing assay and transwell assay, respectively. The cell apoptosis was assessed by flow cytometry assay. Besides, Luciferase reporter assay was employed to examine the interrelation between miR-29a and SNHG20 or DIXDC1.

**RESULTS:** It was demonstrated that SNHG20 and DIXDC1 were significantly upregulated in OSCC tissues and cell lines, while miR-29a was markedly downregulated. Moreover, the high expression of SNHG20 was found to predict a lower survival rate in OSCC patients. In addition, loss-of-function experiments demonstrated that SNHG20 knockdown inhibited the development and progression of OSCC, whereas the miR-29a inhibitor significantly abolished the effect of SNHG20 depletion on OSCC progression by directly binding to SNHG20. DIXDC1 was shown to enhance si-SNHG20 and miR-29a mimic-attenuated cell viability, migration, and invasion by directly binding to miR-29a. Furthermore, it was also found that DIXDC1 activated Wnt signaling in OSCC cells.

**CONCLUSIONS:** Our study demonstrated that SNHG20 promoted OSCC progression via the miR-29a/DIXDC1/Wnt signaling pathway, which might provide a novel theoretical basis for the treatment of OSCC.

*Key Words:*

OSCC, SNHG20, miR-29a, DIXDC1, Wnt signaling.

## Introduction

Oral cavity cancer is a common head and neck malignancy. Squamous cell carcinoma comprises at least 90% of all oral malignancies and accounts for a substantial percentage of cancer-related mortality worldwide<sup>1</sup>. With the development of molecular technologies, a multitude of genes that are frequently involved in cell cycle control, cell survival, and epigenetic regulation have been identified<sup>2</sup>.

Long non-coding RNAs (lncRNAs) are a type of endogenous RNA molecules with a length of > 200 nucleotides. Although lncRNAs do not encode proteins, they often participate in gene regulation and cellular activity by directly interacting with microRNAs (miRNAs)<sup>3</sup>. Several lncRNAs, such as MALAT, PVT1, and TUSC7, are often dysregulated in multiple tumor types<sup>4-6</sup>. Of note, small nucleolar RNA host gene 20 (SNHG20) has been deemed as a potential oncogenic lncRNA in various types of cancer. Chen et al<sup>7</sup> reported that SNHG20 promoted non-small cell lung cancer progression by inhibiting P21 expression. He et al<sup>8</sup> demonstrated that SNHG20 promoted ovarian cancer progression via Wnt/ $\beta$ -catenin signaling. In addition, Wu et al<sup>9</sup> indicated that SNHG20 promoted the tumorigenesis of oral squamous cell carcinoma (OSCC) via the miR-197/lin28 axis. These findings suggested the significant role of SNHG20 in regulating tumor progression. However, the exact mechanisms of SNHG20 in OSCC progression have not been fully explored.

Coiled-coil-DIX1 (Ccd1) has been characterized as a positive regulator of Wnt signaling during embryonic development<sup>10,11</sup>. Xin et al<sup>12</sup> in-

licated that Disheveled-Axin Domain Containing 1 (DIXDC1), a human homolog of Ccd1, caused an increase in the protein levels of the Wnt/ $\beta$ -catenin signaling pathway to promote the growth of acute myeloid leukemia cells. Moreover, Song et al<sup>13</sup> highlighted that miR-514 inhibited the growth and invasion of gastric cancer cells by targeting DIXDC1/Wnt signaling. Based on these findings, we speculated that SNHG20 exerted its oncogenic role by regulating the DIXDC1/Wnt signaling pathway in OSCC progression.

The Wnt/ $\beta$ -catenin signaling pathway has been extensively studied over the last few decades, following its initial discovery as a proto-oncogene (Wnt1) in 1982<sup>14</sup>. This metabolic pathway has been shown to participate in multiple cellular processes, including cell growth, differentiation, development, migration, apoptosis, and genetic stability<sup>15</sup>. In addition, this pathway is highly conserved and often affects tumor progression by regulating the expression levels of specific target genes, such as c-myc, E-cadherin, and cyclin D1<sup>16</sup>. The Wnt/ $\beta$ -catenin signaling pathway has been shown to play a vital role in various types of cancer, such as colorectal, non-small cell lung, gastric, and bladder cancers<sup>17-20</sup>. Recently, Zhao et al<sup>21</sup> demonstrated that the lncRNA SNHG20 promoted bladder cancer progression by regulating the Wnt/ $\beta$ -catenin signaling pathway.

The aim of the present study was to explore the detailed mechanism of the SNHG20-modulated tumorigenesis of OSCC. It was demonstrated that SNHG20 promoted OSCC progression through the miR-29a/DIXDC1/Wnt/ $\beta$ -catenin signaling pathway.

## Patients and Methods

### *Clinical Specimens*

20 paired OSCC tissues and their adjacent normal tissues were obtained from 20 patients aged 30-50 between August 2007 and April 2008. The patients were followed up between May 2008 and June 2015. The study was approved by the Ethics Committee of the Ninth People's Hospital of Shanghai. The subjects provided informed consent for their participation in the study and confirmed that they did not received chemotherapy or radiotherapy prior to surgery.

### *Cell Lines*

The human OSCC cell lines (SCC9, SCC15, and CAL27) and the human normal oral keratino-

cyte (NHOK) cell lines were purchased from the Institute of Biochemistry and Cell Biology of the Chinese Academy of Sciences (Shanghai, China). All cells were cultured at 37°C in a medium consisting of Roswell Park Memorial Institute-1640 (Gibco, Thermo Fisher Scientific, Inc., Waltham, MA, USA) with 10% fetal bovine serum (FBS; Gibco, Thermo Fisher Scientific, Inc., Waltham, MA, USA) in a humidified atmosphere of 5% CO<sub>2</sub>.

### *Plasmids and Transfection*

Small interfering RNAs for the target genes (si-SNHG20-1, si-SNHG20-2), including a scrambled negative control (si-NC), were synthesized by GenePharma (Shanghai, China). NC mimic, miR-29a mimics, NC inhibitor, or miR-29a inhibitor were purchased from GenePharma (Shanghai, China). The transfection was conducted using Lipofectamine 3000 reagent (Invitrogen, Thermo Fisher Scientific, Inc., Waltham, MA, USA), according to the manufacturer's instructions.

### *Luciferase Reporter Assay*

Wild-type or mutant fragments (SNHG20 and DIXDC1) were amplified and integrated into a pGL3 vector (Promega Corporation, Madison, WI, USA). Subsequently, miR-29a mimics, miR-29a inhibitor, and NC were transfected into 293T cells, which had been transfected with wild-type or mutant fragments. Luciferase activity was evaluated by Dual-Luciferase Reporter Analysis system (Promega Corporation, Madison, WI, USA). Firefly Luciferase activity was normalized to Renilla (Promega Corporation, Madison, WI, USA) Luciferase gene activity.

### *Dimethyl Thiazolyl Diphenyl Tetrazolium (MTT) Assay*

The MTT assay was used to detect OSCC cell viability. Transfected cells were seeded in 96-well culture plates (2500 cells/well). Next, 10  $\mu$ L MTT (5 mg/ml; Bioswamp, Wuhan, China) was added and cells were then incubated for 4-6 h. Subsequently, dimethyl sulfoxide (100  $\mu$ L; Bioswamp, Wuhan, China) was added to the wells.

### *Wound Healing Assay*

Cell migration was determined by the wound healing assay, which was conducted following the procedures described by Li et al<sup>22</sup>.

### *Transwell Assay*

OSCC cells ( $1 \times 10^5$ ) were suspended in 200  $\mu$ L of Dulbecco's Modified Eagle's Medium

(DMEM; Gibco, Thermo Fisher Scientific, Inc., Waltham, MA, USA). The mixture was then transferred to the top chamber with Matrigel-coated membrane. Approximately 20% FBS-containing 350  $\mu$ l DMEM media was added to the bottom chamber. The invaded cells were stained with crystal violet for 1-2 h at room temperature. The images were captured using an inverted microscope.

### Flow Cytometry

Transfected cells were rinsed twice with PBS, and then, stained with Annexin V-fluorescein isothiocyanate (Dojindo Molecular Technologies, Inc., Kumamoto, Japan) and propidium iodide (PI; Dojindo Molecular Technologies, Inc., Kumamoto, Japan) in the dark at 37°C for 20 min. Apoptotic cells were analyzed using a flow cytometer (BD Biosciences, Tokyo, Japan).

### Reverse Transcription-Quantitative Polymerase Chain Reaction (RT-qPCR)

Total RNA was extracted from tissues and cells using TRIzol Reagent (Invitrogen, Thermo Fisher Scientific, Inc., Waltham, MA, USA), according to the manufacturer's instructions. The RNAs were reverse transcribed to cDNAs through reverse transcriptase kit (TaKaRa, Dalian, Liaoning, China). RT-qPCR was performed using SYBR-Green PCR Master Mix kit (TaKaRa, Dalian, Liaoning, China). The following amplification conditions were used: pre-denaturation at 95°C for 15 sec, denaturation at 94°C for 30 sec, annealing at 60°C for 20 sec, and extension at 72°C for 40 sec for 40 cycles. The expression levels of the genes were calculated using the  $2^{-\Delta\Delta C_t}$  method. The primer sequences were listed in Table I.

### Western Blot Analysis

Proteins were extracted from transfected OS-CC cells using radioimmunoprecipitation assay buffer (RIPA; Beyotime Institute of Biotechnology, Haimen, China). Protein concentration was measured by the bicinchoninic acid assay (BSA; Beyotime Institute of Biotechnology, Haimen, China). Following denaturing, 10  $\mu$ g protein/lane was separated by 10% SDS-PAGE. Proteins were transferred onto polyvinylidene difluoride (PVDF) membranes and blocked in 5% non-fat milk for 2 h at room temperature. The membranes were incubated with primary antibodies against Wnt3a [1:1,000; Abcam (Cambridge, MA, USA); Cat. No. ab219412],  $\beta$ -catenin [1:1,000; Abcam (Cambridge, MA, USA); Cat. No. ab16051] and GAPDH [1:1,000; Abcam (Cambridge, MA, USA); Cat. No. ab9485] overnight at 4°C. Following primary incubation, the membranes were incubated with horseradish peroxidase-conjugated secondary antibodies [1:1,000; goat anti-mouse IgG, ab205719, and goat anti-Rabbit IgG, ab205718; Abcam (Cambridge, MA, USA)] for 2 h at room temperature. Protein bands were visualized using the Pierce enhanced chemiluminescence (ECL) Western Blotting kit (Pierce; Thermo Fisher Scientific Inc., Waltham, MA, USA). Protein expression was quantified using Image-Pro® Plus software (version 6.0; Media Cybernetics, Inc., Rockville, MD, USA). GAPDH was used as the endogenous control for data normalization.

### Statistical Analysis

The software package Statistical Product and Service Solutions (SPSS) software 22.0 (IBM Corp., Armonk, NY, USA) was used for statistical analysis and each experiment was repeated

**Table I.** The primer sequences used for RT-qPCR analysis.

cDNA	Primer sequences
SNHG20 forward	ATGGCTATAAATAGATACACGC
SNHG20 reverse	GGTACAAACAGGGAGGGA
miR-29a forward	TGCGCTAGCACCATCTGAAAT
miR-29a reverse	GTGCAGGGTCCGAG
DIXDC1 forward	TGCATGTTATGGAGACGCAGAAG
DIXDC1 reverse	AGGTGCTGCTGACAGTTGGAGA
U6 forward	CTCGCTTCGGCAGCACATATACTA
U6 reverse	ACGAATTTGCGTGTTCATCCTTGCG
GAPDH forward	GATGATCTTGAGGCTGTTGTC
GAPDH reverse	CAGGGCTGCTTTTAACTCTG

at least three times. Comparisons of parameters between the two groups were analyzed by a paired Student's *t*-test. The comparisons among multiple groups were performed using one-way ANOVA followed by Tukey's test. Kaplan-Meier analysis and the log-rank test were used to estimate survival curves. Cut-off values were determined using Youden's index.  $p < 0.05$  was considered to indicate a statistically significant difference.

## Results

### *SNHG20 is Upregulated in OSCC and Associated with Poor Prognosis*

To determine the role of SNHG20 in OSCC, 20 OSCC tissues and 20 adjacent normal tissues were collected. The results indicated that the expression of SNHG20 was higher in OSCC tissues than that in normal tissues (Figure 1A). Moreover, the relative expression levels of SNHG20 were measured in three OSCC cell lines (SCC9, SCC15, and CAL27) and one human normal oral keratinocyte cell line (NHOK). RT-qPCR analysis demonstrated that SNHG20 expression was upregulated in OSCC cell lines (Figure 1B). In addition, the association between the SNHG20 expression levels and the overall survival rate was investigated by Kaplan-Meier analysis. The results demonstrated that a higher expression level of SNHG20 was associated with a lower survival rate of OSCC patients (Figure 1C). In conclusion, these results indicated that SNHG20 plays an oncogenic role in OSCC progression.

### *SNHG20 Knockdown Suppresses the Progression of OSCC*

To investigate the effect of SNHG20 on OSCC progression, SCC9 cells were transfected with si-SNHG20-1 and si-SNHG20-2. The depletion of SNHG20 was detected by RT-qPCR (Figure 2A). First, MTT assay demonstrated that the downregulation of SNHG20 resulted in a lower cell viability, as compared with that in the negative control (Figure 2B). Flow cytometry demonstrated that SCC9 cells exhibited a higher apoptotic rate in si-SNHG20-transfected groups than that in the negative control group (Figure 2C). Wound healing and transwell assays indicated that SNHG20 knockdown reduced the migration and invasion abilities of SCC9 cells (Figure 2D and E). In summary, these data showed that SNHG20 depletion significantly inhibited the progression of OSCC.

### *MiR-29a is Involved in SNHG20-Regulated OSCC Progression*

Through bioinformatics analysis, miR-29a was predicted as a potential downstream target of SNHG20 (Figure 3A). It was also found that miR-29a was downregulated in OSCC tissues and OSCC cell lines (Figure 3B and C). The transfection efficiency was indicated by RT-qPCR. The results indicated that the expression of miR-29a was markedly reduced in OSCC cell lines transfected with the miR-29a inhibitor but was notably increased in OSCC cells transfected with miR-29a mimics (Figure 3D). Dual-Luciferase reporter assays revealed that Luciferase activity was significantly inhibited by miR-29a mimics in wild-type SNHG20-transfected 293T

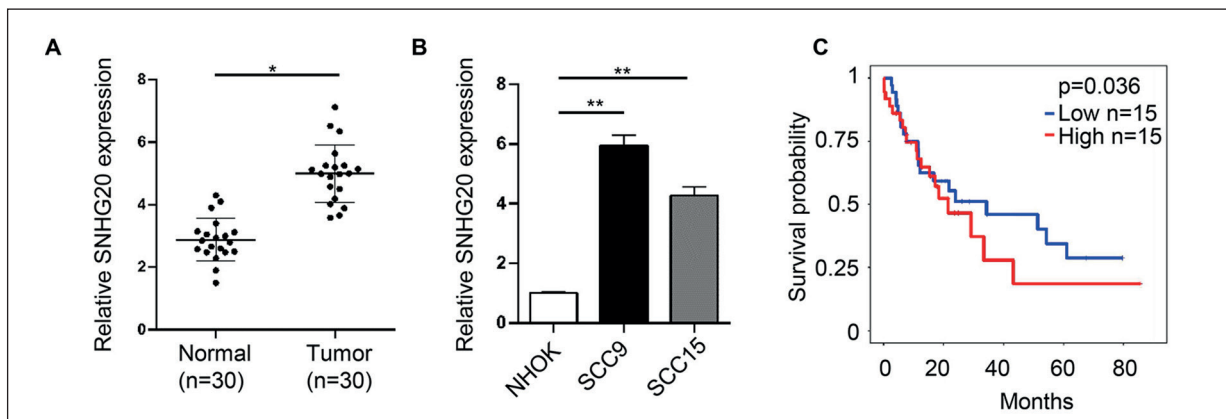


**Figure 1.** SNHG20 is upregulated in OSCC and related to poor prognosis. **A**, The expression level of SNHG20 was examined by RT-qPCR in OSCC tissues (n=20) and the adjacent normal tissues (n=20). **B**, RT-qPCR result of SNHG20 expression level in OSCC cell lines (SCC9, SCC15, and CAL27) and human normal oral keratinocyte cell line (NHOK). **C**, Kaplan-Meier analysis showed the association between SNHG20 expression and the overall survival in OSCC patients.



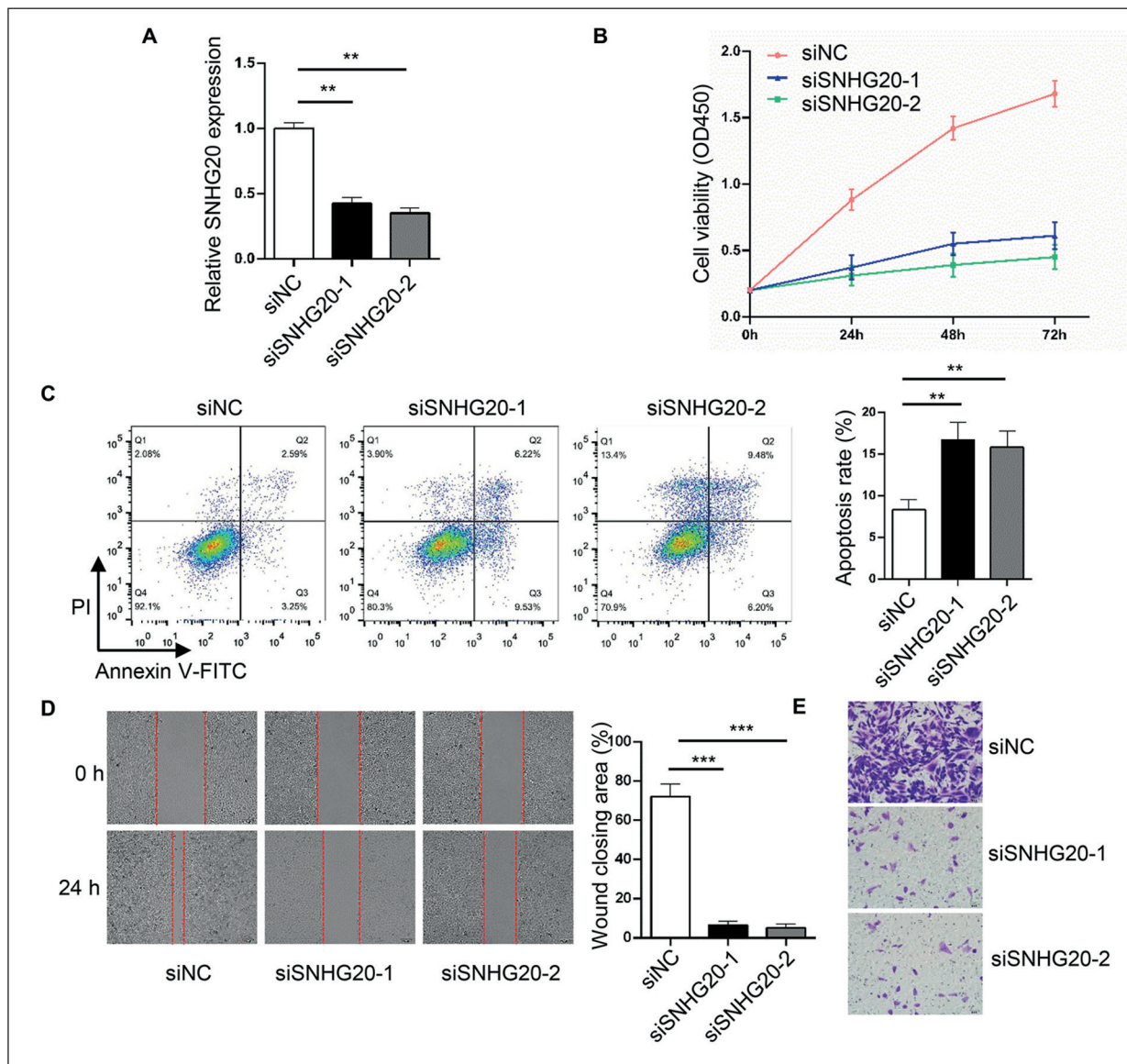


**Figure 2.** SNHG20 knockdown suppresses the progression of OSCC. **A**, RT-qPCR showed SNHG20 expression level in SCC9 cells transfected with si-NC, si-SNHG20-1 or si-SNHG20-2. **B**, MTT showed cell viability of SCC9 cells transfected with si-NC, si-SNHG20-1 or si-SNHG20-2. **C**, Flow cytometry analysis and quantification determined cell apoptosis of SCC9 cells transfected with si-NC, si-SNHG20-1 or si-SNHG20-2. **D**, Wound healing assay and quantification examined cell migration of SCC9 cells transfected with si-NC, si-SNHG20-1 or si-SNHG20-2 (magnification  $\times 200$ ). **E**, Transwell assay detected cell invasion of SCC9 cells transfected with si-NC, si-SNHG20-1 or si-SNHG20-2 (magnification  $\times 200$ ).

cells, whereas it was markedly increased by miR-29a inhibitor (Figure 3E). RT-qPCR confirmed that miR-29a mimics significantly suppressed SNHG20 expression, while the miR-29a inhibitor increased SNHG20 expression (Figure 3F). In addition, we conducted *in vitro* experiments to investigate whether the binding between miR-29a and SNHG20 affects OSCC progression. si-SNHG20 and miR-29a inhibitor were introduced into SCC9 cells. The cell vi-

ability of si-SNHG20 cells was rescued by the introduction of miR-29a inhibitor (Figure 3G). Furthermore, wound healing and transwell assays demonstrated that miR-29a inhibitor significantly reversed si-SNHG20-attenuated migration and invasion activity of SCC9 cells (Figure 3H and I). Taken together, our results showed that miR-29a could directly bind to SNHG20 and reduce its expression levels, leading to the suppression of its oncogenic functions, demon-

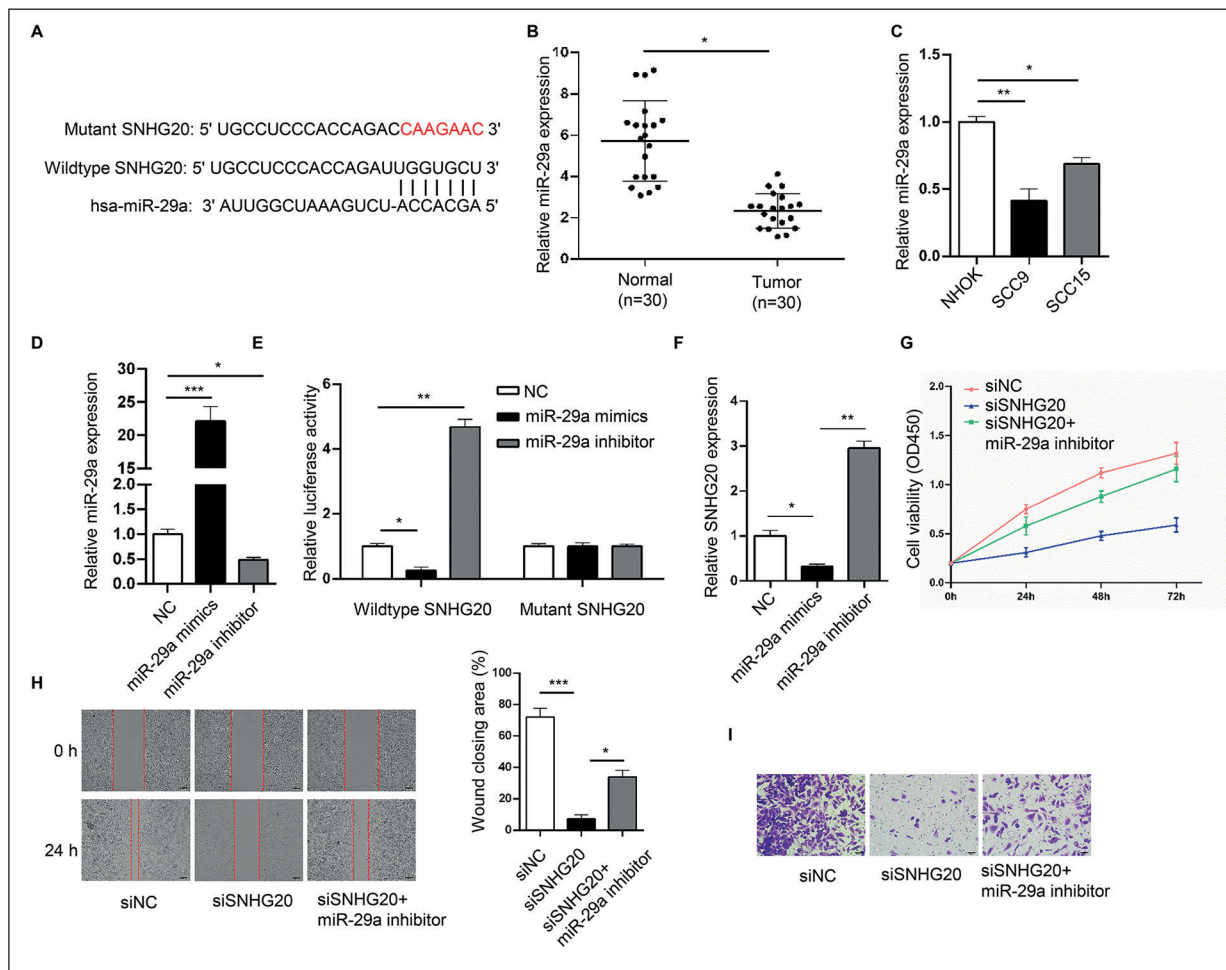


**Figure 3.** MiR-29a is involved in SNHG20-regulated OSCC progression. **A**, The potential binding site between SNHG20 and miR-29a was shown. **B**, MiR-29a expression level was detected by RT-qPCR in OSCC tissues (n=20) and the adjacent normal tissues (n=20). **C**, MiR-29a expression level was detected by RT-qPCR in OSCC cell lines (SCC9, SCC15, and CAL27) and human normal oral keratinocyte cell line (NHOK). **D**, MiR-29a expression level was detected by RT-qPCR in SCC9 cells transfected with NC, miR-29a mimics, and miR-29a inhibitor. **E**, Luciferase activity was examined by Luciferase reporter assay in wildtype or mutant SNHG20-harboring SCC9 cells transfected with negative control (NC), miR-29a mimics, and miR-29a inhibitor. **F**, SNHG20 expression level was detected by RT-qPCR in SCC9 cells transfected with negative control (NC), miR-29a mimics, and miR-29a inhibitor. **G**, MTT showed SCC9 cell viability after transfection of si-NC, si-SNHG20, and si-SNHG20+miR-29a inhibitor. **H**, Wound healing assay and quantification showed SCC9 cell migration after transfection of si-NC, si-SNHG20, and si-SNHG20+miR-29a inhibitor (magnification  $\times 200$ ). **I**, Transwell assay showed SCC9 cell invasion after transfection of si-NC, si-SNHG20, and si-SNHG20+miR-29a inhibitor (magnification  $\times 200$ ).

strating the potential tumor-suppressive function of miR-29a in OSCC progression.

### **Overexpression of DIXDC1 Significantly Abrogates the Inhibitory Effect of si-SNHG20 or miR-29a Mimics on OSCC Progression**

Further investigation focused on the detailed regulatory axis in OSCC by SNHG20/miR-29a. The potential targets for miR-29a were predicted by TargetScan. DIXDC1 was selected from this

screening analysis (Figure 4A). Moreover, RT-qPCR analysis showed that the expression of DIXDC1 was higher in OSCC tissues and cells than that in normal tissues and cells (Figure 4B and C). RT-qPCR analysis further demonstrated that the expression of DIXDC1 was notably increased in OSCC cells transfected with DIXDC1 overexpression plasmid (Figure 4D). Luciferase reporter assays and RT-qPCR analysis indicated the direct interaction between miR-29a and DIXDC1 (Figure 4E and F). MTT, wound healing and



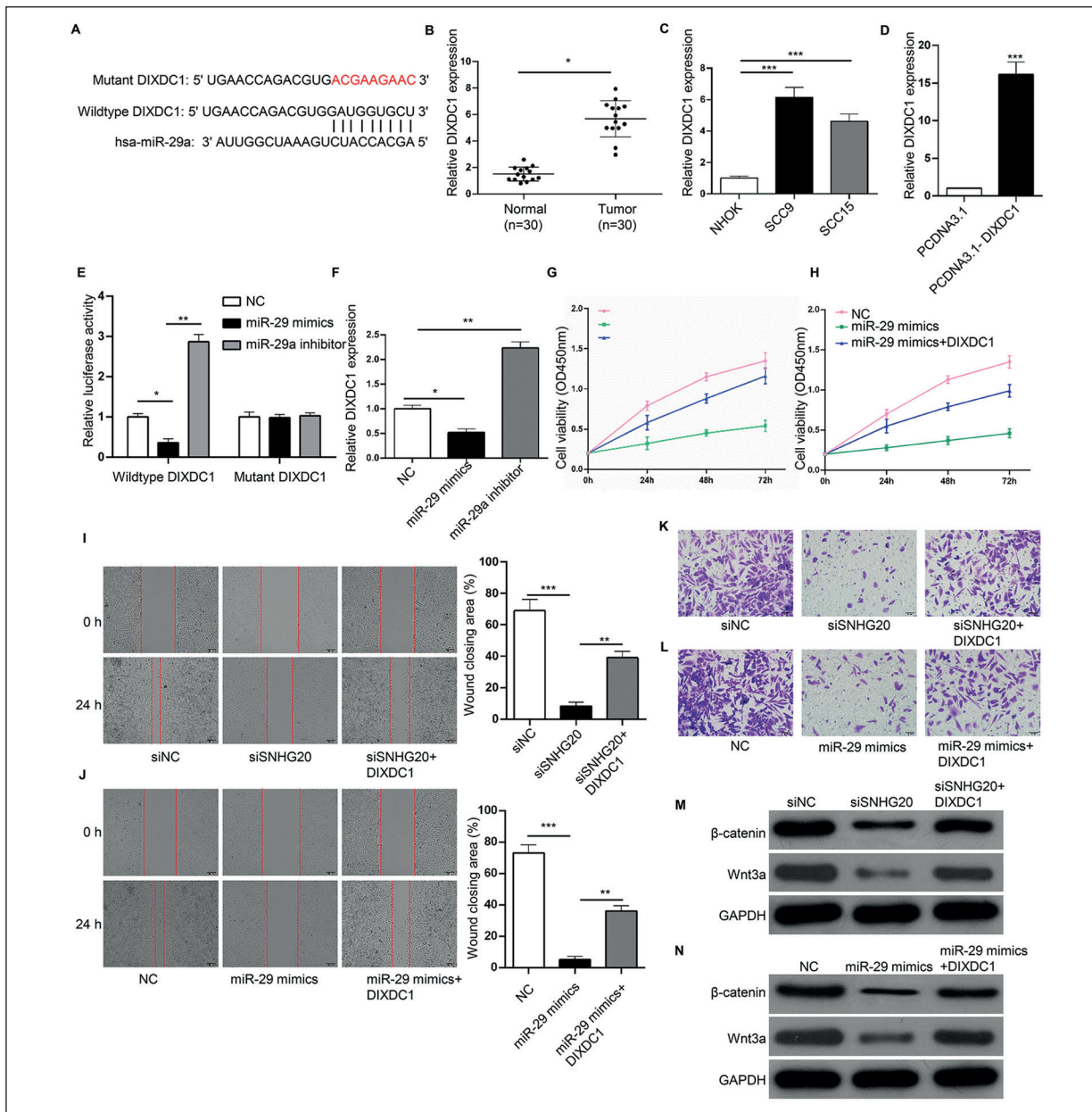


**Figure 4.** Overexpression of DIXDC1 significantly abrogates the inhibitory effect of si-SNHG20 or miR-29a mimics on OSCC progression. **A**, The potential binding site between 3'-UTR of DIXDC1 and miR-29a was shown. **B**, DIXDC1 expression level was detected by RT-qPCR in OSCC tissues (n=20) and the adjacent normal tissues (n=20). **C**, DIXDC1 expression level was detected by RT-qPCR in OSCC cell lines (SCC9, SCC15, and CAL27) and human normal oral keratinocyte cell line (NHOK). **D**, DIXDC1 expression level was detected by RT-qPCR in SCC9 cells transfected with pcDNA3.1 and pcDNA3.1-DIXDC1. **E**, Luciferase activity was examined by luciferase reporter assay in wildtype or mutant 3'-UTR of DIXDC1-harboring SCC9 cells transfected with negative control (NC), miR-29a mimics, and miR-29a inhibitor. **F**, DIXDC1 expression level was detected by RT-qPCR in SCC9 cells transfected with negative control (NC), miR-29a mimics, and miR-29a inhibitor. **G**, MTT showed SCC9 cell viability after transfection of si-NC, si-SNHG20, and si-SNHG20 + DIXDC1. **H**, MTT showed SCC9 cell viability after transfection of NC, miR-29a mimics, and miR-29a mimics + DIXDC1. **I**, Wound healing assay and quantification showed SCC9 cell migration after transfection of si-NC, si-SNHG20, and si-SNHG20 + DIXDC1 (magnification  $\times 200$ ). **J**, Wound healing assay and quantification showed SCC9 cell migration after transfection of NC, miR-29a mimics, and miR-29a mimics + DIXDC1 (magnification  $\times 200$ ). **K**, Transwell assay showed SCC9 cell invasion after transfection of si-NC, si-SNHG20, and si-SNHG20 + DIXDC1 (magnification  $\times 200$ ). **L**, Transwell assay showed SCC9 cell invasion after transfection of NC, miR-29a mimics, and miR-29a mimics + DIXDC1 (magnification  $\times 200$ ). **M**, Western blot analysis showed Wnt3a and  $\beta$ -catenin protein level in SCC9 cells after transfection of si-NC, si-SNHG20, and si-SNHG20 + DIXDC1. **N**, Western blot analysis showed Wnt3a and  $\beta$ -catenin protein level in SCC9 cells after transfection of NC, miR-29a mimics, and miR-29a mimics + DIXDC1.

transwell assays demonstrated that the overexpression of DIXDC1 significantly reversed the si-SNHG20 or miR-29a mimics-attenuated SCC9 cell viability, migration, and invasion, respectively (Figure 4G-L). In addition, Western blot analysis revealed that DIXDC1 overexpression markedly abolished the inhibitory effect of si-SNHG20 or miR-29a mimics on the expression of Wnt3a and  $\beta$ -catenin (Figure 4M and N). Based on these findings, we observed that DIXDC1 acted as a critical effector for SNHG20/miR-29a-regulated OSCC phenotypes by activating the Wnt signaling pathway.

## Discussion

LncRNA has been reported to play a vital role in the development and progression of various tumors. Recent studies<sup>23,24</sup> have shown that SNHG20 participates in multiple pathways to affect cancer progression. However, the investigation of SNHG20 in OSCC remains limited. In the present study, we revealed that SNHG20 was upregulated in OSCC tissues and associated with short overall survival time of OSCC patients. SNHG20 depletion inhibited cell proliferation, migration, and invasion, as well as increased apoptosis rate of OSCC cells.

MiRNAs are a group of small non-coding RNAs that regulate gene expression at the post-transcriptional level. MiR-29a has been reported to function as an oncogene or tumor suppressor in several types of cancers. For example, Wu et al<sup>25</sup> demonstrated that miR-29a was upregulated in breast cancer and its overexpression promoted cell migration and invasion of breast cancer. However, Gong et al<sup>26</sup> revealed that miR-29a was downregulated in cervical cancer tissues and suppressed invasion and metastasis of cervical cancer. In our study, we found that miR-29a expression was reduced in OSCC tissues and OSCC cell lines. Through bioinformatic analysis and Dual-Luciferase reporter assay, we demonstrated miR-29a could directly interact with SNHG20. Moreover, we transfected OSCC cells with NC, miR-29a mimics or miR-29a inhibitor. The results indicated that the upregulation of miR-29a significantly inhibited the expression of SNHG20, which further suppressed the development and progression of OSCC. Subsequently, the bioinformatic analysis and Dual-Luciferase reporter assay revealed that DIXDC1 was a downstream

target of miR-29a. Moreover, we found that DIXDC1 was upregulated in OSCC tissues and cells and its overexpression reverted the attenuated cell proliferation, migration, and invasion of OSCC caused by depletion of SNHG20 or overexpression of miR-29a. Therefore, we demonstrated that SNHG20 acted as a competing endogenous RNA (ceRNA) to sponge miR-29a to promote the development and progression of OSCC *via* upregulating DIXDC1.

Previous studies<sup>27-29</sup> have shown that lncRNAs affect tumor cell proliferation *via* the Wnt/ $\beta$ -catenin signaling pathway. This pathway has been reported to participate in the regulation of OSCC migration and invasion<sup>30</sup>. Liang et al<sup>31</sup> evaluated that TUG1 regulated OSCC progression *via* the Wnt/ $\beta$ -catenin signaling pathway. Our results demonstrated that SNHG20 depletion and miR-29a mimics led to the reduction of  $\beta$ -catenin expression. The data determined that abnormal expression of SNHG20 or miR-29a in OSCC cells indeed resulted in aberrant Wnt signaling activity, thereby regulating OSCC progression.

## Conclusions

Our study showed that SNHG20 contributed to OSCC by sponging miR-29a, and then, modulated the DIXDC1/Wnt pathway. Our findings provide a novel theoretical basis for the treatment of OSCC.

## Conflict of Interest

The Authors declare that they have no conflict of interests.

## References

- 1) MASSANO J, REGATEIRO FS, JANUÁRIO G, FERREIRA A. Oral squamous cell carcinoma: review of prognostic and predictive factors. *Oral Surg Oral Med Oral Pathol Oral Radiol Endod* 2006; 102: 67-76.
- 2) LEEMANS CR, SNIJDERS PJ, BRAKENHOFF RH. The molecular landscape of head and neck cancer. *Nat Rev Cancer* 2018; 18: 269-282.
- 3) YAMAMURA S, IMAI-SUMIDA M, TANAKA Y, DAHIYA R. Interaction and cross-talk between non-coding RNAs. *Cell Mol Life Sci* 2018; 75: 467-484.
- 4) LIANG J, LIANG L, OUYANG K, LI Z, YI X. MALAT 1 induces tongue cancer cells' EMT and inhibits apoptosis through Wnt/ $\beta$ -catenin signaling pathway. *J Oral Pathol Med* 2017; 46: 98-105.



- 5) FAN H, ZHU JH, YAO XO. Long non-coding RNA PVT1 as a novel potential biomarker for predicting the prognosis of colorectal cancer. *Int J Biol Marker* 2018; 1724600818777242.
- 6) WANG P, XU J, WANG Y, CAO X. An interferon-independent lncRNA promotes viral replication by modulating cellular metabolism. *Science* 2017; 358: 1051-1055.
- 7) CHEN Z, CHEN X, CHEN P, YU S, NIE F, LU B, ZHANG T, ZHOU Y, CHEN Q, WEI C, WANG W, WANG Z. Long non-coding RNA SNHG20 promotes non-small cell lung cancer cell proliferation and migration by epigenetically silencing of P21 expression. *Cell Death Dis* 2017; 8: e3092-e3092.
- 8) HE S, ZHAO Y, WANG X, DENG Y, WAN Z, YAO S, SHEN H. Up-regulation of long non-coding RNA SNHG20 promotes ovarian cancer progression via Wnt/ $\beta$ -catenin signaling. *Biosci Rep* 2018; 38: BSR20170681.
- 9) WU J, ZHAO W, WANG Z, XIANG X, ZHANG S, LIU L. Long non-coding RNA SNHG20 promotes the tumorigenesis of oral squamous cell carcinoma via targeting miR-197/LIN28 axis. *J Cell Mol Med* 2019; 23: 680-688.
- 10) SOMA K, SHIOMI K, KEINO-MASU K, MASU M. Expression of mouse Coiled-coil-DIX1 (Ccd1), a positive regulator of Wnt signaling, during embryonic development. *Gene Expr Patterns* 2006; 6: 325-330.
- 11) SHIOMI K, KANEMOTO M, KEINO-MASU K, YOSHIDA S, SOMA K, MASU M. Identification and differential expression of multiple isoforms of mouse Coiled-coil-DIX1 (Ccd1), a positive regulator of Wnt signaling. *Mol Brain* 2005; 135: 169-180.
- 12) XIN H, LI C, WANG M. DIXDC1 promotes the growth of acute myeloid leukemia cells by upregulating the Wnt/ $\beta$ -catenin signaling pathway. *Biomed Pharmacother* 2018; 107: 1548-1555.
- 13) SONG J, GUAN Z, LI M, SHA S, SONG C, GAO Z, ZHAO Y. MicroRNA-154 inhibits the growth and invasion of gastric cancer cells by targeting DIXDC1/WNT signaling. *Oncol Res* 2018; 26: 847-856.
- 14) NUSSE R, VARMIUS HE. Many tumors induced by the mouse mammary tumor virus contain a provirus integrated in the same region of the host genome. *Cell* 1982; 31: 99-109.
- 15) NUSSE R, CLEVERS H. Wnt/ $\beta$ -catenin signaling, disease, and emerging therapeutic modalities. *Cell* 2017; 169: 985-999.
- 16) ANASTAS JN, MOON RT. WNT signalling pathways as therapeutic targets in cancer. *Nat Rev Cancer* 2013; 13: 11-26.
- 17) HU TH, YAO Y, YU S, HAN LL, WANG WJ, GUO H, TIAN T, RUAN ZP, KANG XM, WANG J, WANG SH, NAN KJ. SDF-1/CXCR4 promotes epithelial-mesenchymal transition and progression of colorectal cancer by activation of the Wnt/ $\beta$ -catenin signaling pathway. *Cancer Lett* 2014; 354: 417-426.
- 18) LI L, WANG QF, ZOU ML, HE XA, LV JJ. Overexpressed lncRNA ZEB1-AS1 promotes cell invasion and angiogenesis through Wnt/ $\beta$ -catenin signaling in non-small cell lung cancer. *Int J Clin Exp Pathol* 2017; 10: 3990-3997.
- 19) PENG Y, ZHANG X, MA Q, YAN R, QIN Y, ZHAO Y, CHENG Y, YANG M, WANG Q, FENG X, HUANG Y, HUANG W, ZHAO Z, WANG L, WEI Y, HE Z, FAN X, LI S, JIN Z, MELTZER SJ. MiRNA-194 activates the Wnt/ $\beta$ -catenin signaling pathway in gastric cancer by targeting the negative Wnt regulator, SUFU. *Cancer Lett* 2017; 385: 117-127.
- 20) URAKAMI S, SHIINA H, ENOKIDA H, KAWAKAMI T, TOKIZANE T, OGISHIMA T, TANAKA Y, LI L-C, RIBEIRO-FILHO LA, TERASHIMA M, KIKUNO N, ADACHI H, YONEDA T, KISHI H, SHIGENO K, KONETY BR, IGAWA M, DAHIYA R. Epigenetic inactivation of Wnt inhibitory factor-1 plays an important role in bladder cancer through aberrant canonical Wnt/ $\beta$ -catenin signaling pathway. *Clin Cancer Res* 2006; 12: 383-391.
- 21) ZHAO Q, GAO S, DU Q, LIU Y. Long non-coding RNA SNHG20 promotes bladder cancer via activating the Wnt/ $\beta$ -catenin signalling pathway. *Int J Mol Med* 2018; 42: 2839-2848.
- 22) LI C, ZHOU L, HE J, FANG XQ, ZHU SW, XIONG MM. Increased long noncoding RNA SNHG20 predicts poor prognosis in colorectal cancer. *BMC cancer* 2016; 16: 655.
- 23) LIU J, LIU L, WAN JX, SONG Y. Long noncoding RNA SNHG20 promotes gastric cancer progression by inhibiting p21 expression and regulating the GSK-3/ $\beta$ -catenin signaling pathway. *Oncotarget* 2017; 8: 80700-80708.
- 24) GUAN YX, ZHANG MZ, CHEN XZ, ZHANG Q, LIU SZ, ZHANG YL. Lnc RNA SNHG20 participated in proliferation, invasion, and migration of breast cancer cells via miR-495. *J Cell Biochem* 2018; 119: 7971-7981.
- 25) WU Y, SHI W, TANG T, WANG Y, YIN X, CHEN Y, ZHANG Y, XING Y, SHEN Y, XIA T, GUO C, PAN Y, JIN L. MiR-29a contributes to breast cancer cells epithelial-mesenchymal transition, migration, and invasion via down-regulating histone H4K20 trimethylation through directly targeting SUV420H2. *Cell Death Dis* 2019; 10: 1-16.
- 26) GONG Y, WAN JH, ZOU W, LIAN GY, QIN JL, WANG QM. MiR-29a inhibits invasion and metastasis of cervical cancer via modulating methylation of tumor suppressor SOCS1. *Future Oncol* 2019; 15: 1729-1744.
- 27) FAN Y, SHEN B, TAN M, MU X, QIN Y, ZHANG F, LIU Y. Long non-coding RNA UCA1 increases chemoresistance of bladder cancer cells by regulating Wnt signaling. *FEBS J* 2014; 281: 1750-1758.
- 28) WANG G, LI Z, ZHAO Q, ZHU Y, ZHAO C, LI X, MA Z, LI X, ZHANG Y. LincRNA-p21 enhances the sensitivity of radiotherapy for human colorectal cancer by targeting the Wnt/ $\beta$ -catenin signaling pathway. *Oncol Rep* 2014; 31: 1839-1845.
- 29) MA Y, YANG Y, WANG F, MOYER M-P, WEI Q, ZHANG P, YANG Z, LIU W, ZHANG H, CHEN N, WANG H, WANG

- H, QIN H. Long non-coding RNA CCAL regulates colorectal cancer progression by activating Wnt/ $\beta$ -catenin signalling pathway via suppression of activator protein 2 $\alpha$ . *Gut* 2016; 65: 1494-1504.
- 30) IWAI S, YONEKAWA A, HARADA C, HAMADA M, KATAGIRI W, NAKAZAWA M, YURA Y. Involvement of the Wnt- $\beta$ -catenin pathway in invasion and migration of oral squamous carcinoma cells. *Int J Oncol* 2010; 37: 1095-1103.
- 31) LIANG S, ZHANG S, WANG P, YANG C, SHANG C, YANG J, WANG J. LncRNA, TUG1 regulates the oral squamous cell carcinoma progression possibly via interacting with Wnt/beta-catenin signaling. *Gene* 2017; 608: 49-57.